

Brain-Controlled Interfaces: Movement Restoration with Neural Prosthetics

Review

Andrew B. Schwartz,^{1,*} X. Tracy Cui,²
Douglas J. Weber,³ and Daniel W. Moran⁴

¹Departments of Neurobiology and Bioengineering
Center for the Neural Basis of Cognition
McGowan Institute for Regenerative Medicine

²Department of Bioengineering
McGowan Institute for Regenerative Medicine

³Departments of Physical Medicine and Rehabilitation
and Bioengineering

The University of Pittsburgh
Pittsburgh, Pennsylvania 15213

⁴Departments of Biomechanical Engineering
and Neurobiology

Washington University
St. Louis, Missouri 63130

Brain-controlled interfaces are devices that capture brain transmissions involved in a subject's intention to act, with the potential to restore communication and movement to those who are immobilized. Current devices record electrical activity from the scalp, on the surface of the brain, and within the cerebral cortex. These signals are being translated to command signals driving prosthetic limbs and computer displays. Somatosensory feedback is being added to this control as generated behaviors become more complex. New technology to engineer the tissue-electrode interface, electrode design, and extraction algorithms to transform the recorded signal to movement will help translate exciting laboratory demonstrations to patient practice in the near future.

From the rapid growth in biotechnology, neural engineering has emerged as a new field. The merger of systems neurophysiology and engineering has resulted in approaches to link brain activity with man-made devices to replace lost sensory and motor function. The excitement in this field is based not only on the prospect of helping a wide range of patients with neural disorders, but also on the certainty that this new technology will make it possible to gain scientific insight into the way populations of neurons interact in the complex, distributed systems that generate behavior. This review will address recent progress in cortical motor prosthetics. Related reviews are also available (Schwartz, 2004; Wilson et al., 2006; Lebedev and Nicolelis, 2006; Leuthardt et al., 2006).

Neural prosthetics are devices that link machines to the nervous system for the purpose of restoring lost function. Two broad approaches are used in this field: neurons are stimulated or inhibited by applied current, or their activity is recorded to intercept motor intention. Stimulation can be used for its therapeutic efficacy, as in deep brain stimulation to ameliorate the symptoms of Parkinson's disease or to communicate input to the nervous system (for example by transforming sound to

neural input with cochlear prosthetics). In contrast, recordings are used to decode ongoing activity for use as a command or input signal to an external device. Capturing motor intention and executing the desired movement form the basis of brain-controlled interfaces (BCI), a subset of neural prosthetics used to decode intention in order to restore motor ability or communication to impaired individuals.

Every BCI has four broad components: recording of neural activity; extraction of the intended action from that activity; generation of the desired action with a prosthetic effector; and feedback, either through intact sensation, such as vision, or generated and applied by the prosthetic device (Figure 1).

Recording Technology

The first step in the BCI process is to capture signals containing information about the subject's intended movement. While researchers have envisioned using methods based on either magnetic (Georgopoulos et al., 2005) or electromagnetic (Weiskopf et al., 2004; Yoo et al., 2004) signals from the brain, these devices are not yet practical for BCI use. Currently, the four primary recording modalities are electroencephalography (EEG), electrocorticography (ECoG), local field potentials (LFPs), and single-neuron action potential recordings (single units). All of these methods record microvolt-level extracellular potentials generated by neurons in the cortical layers. The methods are classified by whether the electrodes are placed on the scalp, dura, cortical surface, or in the parenchyma, and by the spatial and spectral frequency of their recorded signals. Generally, there is a tradeoff between these parameters; the more invasive the recording technique, the higher the spatial/spectral frequency content of the recorded signal which, in turn, depends on the current densities conducted through the volume of the head. The primary current sources and sinks, i.e., where current enters the cell and leaves the cell, respectively, are synapses (both excitatory and inhibitory) and the voltage-sensitive gates underlying neuronal action potentials. Because most nonspherical neurons are oriented radially, these currents approximate a dipole source, which contains both equal and opposite polarities, oriented perpendicular to the cortical surface. Taken as a whole, the cortex can be modeled as a thin, convoluted sheet of aligned dipoles whose individual magnitudes vary continuously in time. BCI recording aims to sample this dipole sheet and extract the desired control signal.

From a purely engineering point of view, the optimal method of recording this electrical information would be to place a series of small electrodes directly into the dipole sheet to intercept signals from individual neurons (single-unit BCI designs). The ability of a microelectrode to record single-unit action potentials depends on many factors, such as electrode impedance, tip size and shape, whether the target cell has an open or closed extracellular field, and the size and orientation of the target neuron. Layer V cells in the motor cortex have the largest

*Correspondence: abs21@pitt.edu

Extraction Algorithm

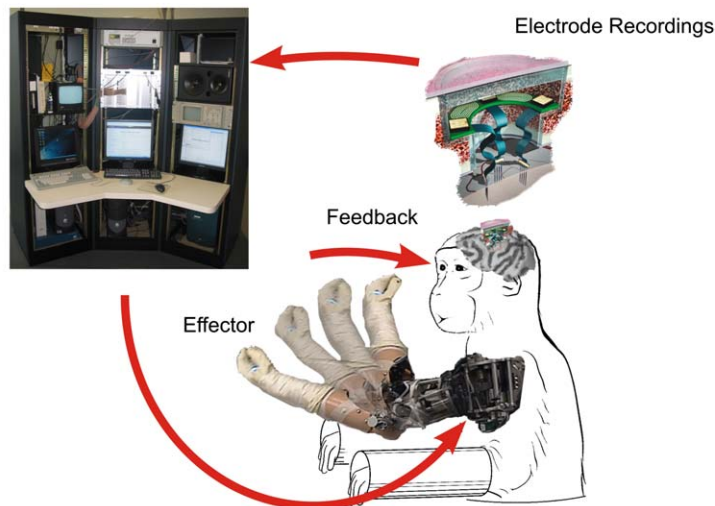


Figure 1. BCI Schematic

Neural activity recorded from the brain is transmitted to a processor that operates an extraction algorithm on the recorded signal. The extracted control signal is fed to a robot controller to move the prosthetic arm, which generates feedback to close the control loop. Electrode inset courtesy of Daryl Kipke, University of Michigan.

cell bodies in the cerebrum ($>100 \mu\text{m}$) and generate large electrical fields, making them an ideal source for extracellular recording. Multisite silicon probes can record distinguishable spikes from layer V neurons in rat sensorimotor cortex located more than $300 \mu\text{m}$ away in the axial direction (Buzsaki and Kandel, 1998), although this distance is likely smaller in the tangential direction (Henze et al., 2000). At this spatial resolution, the potentials due to local synaptic currents are negligible compared to the electric potentials created by an action potential. These signals are usually band-pass filtered from 300 to 10,000 Hz and then passed through a spike discriminator to measure spike time occurrences. As will be discussed later, the firing rates of individual neurons are computed in 10–20 ms bins and “decoded” to provide a high-fidelity prediction of either computer cursor or robot endpoint kinematics. Given its high spatial resolution ($100 \mu\text{m}$) as well as its high temporal resolution (50–100 Hz), this modality arguably provides the highest level of control in BCI applications. One problem with this technique is that, once the electrodes penetrate the parenchyma, they are susceptible to a number of failure modes (see below). Alternatively, recent work using ECoG and LFPs suggests that some spike-related activity can be extracted by looking at higher frequencies and that this signal may provide reasonable BCI control.

EEG

Common wisdom holds that EEG is the safest way of recording brain activity because the electrodes are placed on the scalp. Unfortunately, the human scalp is 2–3 cm away from the surface of the cortex. Given that the potential from an individual dipole falls off at one over the square of distance, a 300 microvolt action potential, recorded $100 \mu\text{m}$ away from a neuron, would fall to an amplitude of 25 picovolts when recorded 2 cm away (Figure 2). Therefore, EEG signals are generated from a large neuronal population of synchronously active neurons. The polarity of the component dipoles, at any given instant of time, match and constructively sum across the population. In general, for real-time signal acquisition (i.e., no averaging), it has been estimated that

nearly 6 cm^2 of cortical tissue must be synchronized in order to produce a measurable scalp potential on the order of a few microvolts (Cooper et al., 1965; Ebersole, 1997; Nunez and Srinivasan, 2006). Given that the standard pyramidal cell orientation yields electrical dipoles perpendicular to the cortical surface, the dominant potentials seen in EEG come from the underlying gyrus rather than cortical sulcal tissue. Likewise, given the average density of neurons in neocortical tissue, a person using EEG to control a BCI device in real time must learn to synchronously modulate the activity of at least 100 million gyral neurons, which is why EEG can only resolve low spatial frequencies.

Because EEG is noninvasive, it has historically dominated BCI research, especially in human subjects. Researchers have used spontaneous activity such as slow cortical potentials (Elbert et al., 1980) or

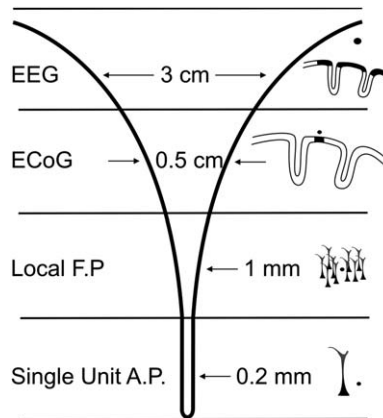


Figure 2. Comparisons of the Spatial Domains of the Four Primary Electrical Recording Modalities for Brain Computer Interfaces

A typical EEG electrode (black circle) located $\sim 2 \text{ cm}$ above the cortex averages gyral neural activity across a 3 cm spatial extent (filled black cortical layers). ECoG electrodes lie just above the cortex and average neural activity over a smaller 0.5 cm range. Both local field potentials and single-unit action potentials are recorded from within the brain parenchyma and sample even smaller areas of neural tissue, yielding higher spatial resolutions.

sensorimotor rhythms (Niedermeyer and Lopes da Silva, 1999) as well as evoked activity such as the P300 (Donchin and Smith, 1970) for control. Slow cortical potentials are generally recorded in the time domain over the vertex of the head. The temporal frequency content of these signals is low (<1 Hz), since they take on the order of a few seconds to occur. Nonetheless, slow cortical potentials have been used successfully in both control volunteers (intact) and motor-impaired patients for BCI control (Birbaumer et al., 1999; Kubler et al., 2001). Evoked activity, such as the P300 wave recorded over parietal cortex, is also an EEG signal in the time domain. In paradigms using this approach, the BCI system rapidly flashes letters to the user via a computer monitor. When the desired letter appears on the screen, a significant peak in the EEG waveform appears 300 ms later. By incorporating an automatic peak detector, a simple yet effective computer spelling system can be used by motor-impaired individuals (Donchin and Smith, 1970; Donchin et al., 2000; Sellers and Donchin, 2006). Given the inherent 300 ms delay between stimulus presentation and EEG activity, the P300, like slow cortical potentials (SCP), also has low temporal frequency content.

Unlike the purely temporal analysis of EEG signals in SCP and P300 systems, the use of sensorimotor rhythms for BCI control is essentially a time-frequency analysis. By analyzing the temporal change in power of multiple independent frequencies bands within an EEG signal, control of multiple dimensions can be carried out with the same recording electrode. Although spiking activity of individual neurons generates extracellular potentials with frequency components up to 5–10 kHz, the EEG signal on the surface of the brain does not contain significant frequency content above 70 Hz. A combination of factors effectively “low-pass filter” the underlying cortical activity. For instance, the large distance between the recording electrode and the underlying cortex allows capacitive effects of the tissue to shunt high-frequency currents more locally. Likewise, modeling results suggest that high-frequency reductions in the dipole moments as a function of distance significantly add to this effect (Nunez and Srinivasan, 2006).

Mu (8–12 Hz) and beta (18–25 Hz) frequencies are the two dominant bands used in EEG BCI (McFarland et al., 2000). During movement, these two frequency bands show a significant decrease in power, indicating that the underlying cortical activity has “desynchronized” during movement. Furthermore, this desynchronization appears during imagined movements as well, suggesting that individuals without muscle control can still modulate these frequency bands (Pfurtscheller and Neuper, 1997). In fact, subjects with spinal cord injury and ALS have successfully learned to modulate the amplitude of these sensorimotor rhythms for simple BCI control of one- and two-dimensional computer cursors, as well as a hand orthosis (Wolpaw and McFarland, 2004; Kubler et al., 2005).

ECoG

One of the major limitations of EEG-based BCI systems is the large distances between the recording electrodes on the surface of the scalp and the underlying cortical tissue (2–3 cm). As discussed above, the spatial frequency of this signal makes it difficult to obtain multiple independent areas of control in, for instance, motor

cortical regions. The advantage of ECoG-based BCI systems is that recording electrodes are approximated on the cortical surface, yielding a much finer spatial resolution on the order of mm (Freeman et al., 2003) as well as the ability to record higher-frequency (10–200 Hz) content in the signal (Leuthardt, et al., 2004; Pfurtscheller et al., 2003).

ECoG BCI research has almost exclusively been performed on human epilepsy patients, in whom subdural grids are clinically placed over suspected epileptogenic foci. These patients are clinically monitored for a period of 1–2 weeks before the ECoG grids are removed, allowing researchers several opportunities to test both the finer spatial resolution and higher spectral frequency of this signal.

A study by Leuthardt et al. (2004) showed that patients could quickly learn to modulate high-frequency gamma rhythms in both motor cortical areas and in Broca’s speech area to control a one-dimensional computer cursor in real time. A subsequent study by this group has shown two-dimensional (2D) control of a computer cursor using the upper arm region of motor cortex for one dimension and the hand region for the other dimension (Schalk et al., 2004). Recently, another BCI ECoG group has used high gamma activity from auditory regions of cortex, showing that subjects can volitionally modulate activity in widespread cortical regions (Wilson et al., 2006). One of the most interesting findings from these studies is that the higher gamma frequencies can be quickly modified through biofeedback to improve both the accuracy and speed of the resulting movement. While ECoG systems are invasive, it is believed that, because they are on the brain surface, they are more robust than penetrating electrodes and therefore should be more durable (Margalit et al., 2003). ECoG electrodes suitable for chronic implants are just now being developed and will soon be tested in nonhuman primates.

LFPs

The signals from penetrating microelectrodes used in single-unit recordings are typically band-pass filtered between 300 and 5000 Hz; however, the same electrodes can be used to record lower-frequency (<250 Hz) LFPs. Recording this band may be advantageous because the lower-frequency components are believed to be much less affected by geometry, and the tissue-electrode interface so critical for single-unit recordings. Most of the earlier studies using LFPs for control have concentrated on temporal analysis. A study by Kennedy using cone electrodes implanted in the motor cortex of a “locked-in” subject demonstrated that LFPs can be used to control a computer cursor in two directions along a single dimension (Kennedy et al., 2004). Several studies in nonhuman primates have used field potential recordings in motor cortex. For instance, Rickert et al. (2005) found limited LFP temporal tuning to movement direction during a 2D center-out reaching task. Unfortunately, time domain analyses of LFPs have not provided nearly the level of elegant control obtained from single-unit recordings.

Recent LFP studies using frequency domain analyses show very promising results for BCI control. Most of the earlier studies concentrated on the lower frequencies apparent in EEG signals. Sanes and Donoghue observed desynchronization in the 15–35 Hz range similar

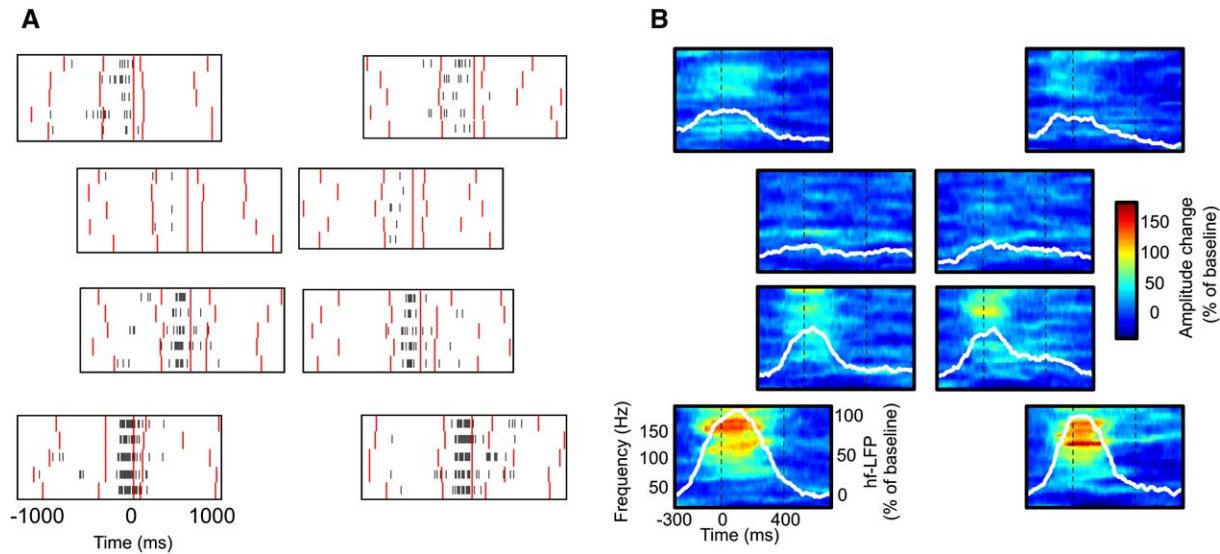


Figure 3. Relationship between Single-Unit Action Potential Activity and Local Field Potential Spectral Power
(A) Spike raster plots during a classic 3D center-out reaching task. The four inner plots represent reaches to the four targets farthest from the subject, while the four outer plots represent reaches to the four targets closest to the subject. The neural activity of this neuron is “tuned” for movements downward and toward the subject (i.e., the bottom two targets have the largest single unit activity).
(B) LFP spectral amplitude as a percentage change from baseline of the LFP recorded on the same electrode. The white line represents the average spectral amplitude of the LFP from 60 to 200 Hz. The average power between 60 and 200 Hz is similarly cosine tuned to movement direction. Furthermore, its temporal profile is well correlated to the speed profile of the hand, suggesting that both single-unit activity and high-frequency local field potentials in motor cortex encode movement velocity (modified from Heldman et al., 2006).

to the mu and beta rhythms of EEG (Sanes and Donoghue, 1993), while in another study, they found an increase in power in the 35–50 Hz range (Sanes and Donoghue, 1993; Donoghue et al., 1998). Andersen and colleagues have found increases in low gamma band activity (35–70 Hz) in parietal cortex during the memory period of a reaching and saccade task (Scherberger et al., 2005) and have highlighted the benefits of using LFPs for BCI applications (Andersen et al., 2004). Given the recent success in using high gamma band activity (100–200 Hz) in ECoG BCI studies, a few groups have analyzed these bands in LFP recordings and found that these frequencies show significant cosine tuning to movement direction in both 2D and 3D center-out reaching tasks (Heldman et al., 2004, 2006; Rickert et al., 2005). In the study by Heldman et al. (Figure 3), the high-frequency band-tuning of LFPs was significantly correlated to the tuning of simultaneously recorded single units, suggesting that these frequencies contain significant power from action potentials in addition to the synaptic activity that is hypothesized to dominate the lower frequencies. If the high gamma band activity in LFPs is well correlated to single-unit activity and robust in the chronic setting, they may provide an accurate control signal for neuroprosthetic applications in the future.

Single Units

Action potentials from single neurons are recorded extracellularly with microelectrodes. Spike waveforms representing action potentials and recorded simultaneously from many individual neurons contain information that can be used to generate elaborate arm movement. In prosthetic applications, many of these electrodes are implanted permanently in the cerebral

cortex. The electrodes typically have 10–50 μm tips, shanks that are 1–5 mm in length, and one or more conductors surrounded by insulation. At the end of the shank or along its length are exposed, conductive recording sites. Conductive leads are routed from the electrode shanks to exit the brain. Access to the cortical surface is gained by removing a small piece of skull (typically about 2 cm) and the dura matter over the exposed brain. After the electrodes are implanted, the leads are led out through the lumen to either a skull-mounted connector or to a telemetry device. The lumen is then sealed, and in the future, telemetry devices will make it possible to close the scalp completely. Most current chronic microelectrodes used in BCI are either micro-wires or microfabricated silicon arrays.

Microwires. Microwires are the oldest form of chronic microelectrodes (Salzman and Bak, 1973; Schmidt et al., 1976; Schmidt, 1999). Typically they are 30–50 μm in diameter, with a core of stainless steel or tungsten insulated with Teflon or polyimide (Williams et al., 1999a; Nicolelis et al., 2003). Arrays are arranged in multiple rows, with eight or more wires spaced 200–300 μm apart. The configuration is held together with polyethylene glycol or methyl methacrylate. The tips are cut with scissors to the same length and may then be polished and beveled; the opposite end of each wire is soldered to a microconnector. New versions of these arrays are made with laser technology (Tucker-Davis Technologies; <http://www.tdt.com/>) or employ a circuit board for denser connections (Nicolelis et al., 2003). Arrays are placed through the reflected dura with a micromanipulator into the exposed cortical surface. The strategy used to implant these devices is to insert them very slowly (100 μm/min) to minimize compression of the

cortex, as the closely spaced, relatively blunt probes do not pass easily into the parenchyma. We have found that insertion depths of about 2 mm seem to result in the highest number of discernable spike waveforms in macaque motor cortex. Once inserted to the desired depth, the wires, along with the connector, are cemented to the exposed skull. The exposed cortex is covered with cellulose foam and sealed with methyl methacrylate. Although the brain can move relative to the skull-fixed arrays—with potential damage to the tissue around the probes—these devices have had long-term success in our laboratory (more than 5 years) and in others (Williams et al., 1999a; Nicolelis et al., 2003). However, typical results show that only about half the implanted wires yield recordable units. This may be due to placement of the electrode tips (i.e., planar arrangement in a curved cortex; dimpling of the cortex during insertion and subsequent rebound of the cortical layers, leaving the tips in the white matter; general cortical trauma due to the electrodes; and chronic inflammation around the implant). Many of these issues are common to all types of micro-electrode implantation and will be addressed below.

Planar Silicon Arrays. Planar recording probes fabricated with photolithography have been developed in the last 20 years (Najafi et al., 1985; Vetter et al., 2004; Moxon et al., 2004b). Of these, a good example comes from the University of Michigan. Fabrication begins with boron diffusion of the silicon wafer to delineate the shape of the probe. A number of steps are used to deposit silicon dioxide and silicon nitride insulation, followed by photolithography to pattern the interconnects and recording sites. As a final step, iridium is layered over the exposed recording sites. This approach allows for a wide variety of probe shapes and configurations. A standard probe consists of four dagger-like shanks 15 μm thick, 50–100 μm wide, and spaced 150 μm apart. The interconnects, running up the parallel shanks, are connected to a microsilicon ribbon cable that is flexible (in one dimension) and has a connector at the end. The design for monkey recording is 3.8 mm long and has four recording shafts placed along each shaft. Probes are implanted with a pair of forceps through the reflected dura. In contrast to microwires, the semiflexible ribbon cable allows the probes to “float” in the brain, moving up and down with the cortex as it pulses. Since the multiple recording sites are placed along the shaft, at least some of the sites are likely to be situated at cortical depths desirable for good extracellular recordings. We commonly record units on almost all sites of these probes in the first few days after surgery. This time course differs from the common pattern seen with microwires, where it may take weeks for a good number of units to appear (Nicolelis et al., 2003). However, as with all chronic probes, the recorded signal deteriorates over the life span of the implant. These probes are currently available though NeuroNexus Technologies (<http://www.neuronexustech.com/>). New design features include fluid channels for delivery of bioactive molecules through the probes, perforated shanks through which neurites will grow, more flexible ribbon cables, and stacking of the arrays to form 3D structures.

Three-Dimensional Silicon Arrays. In contrast to the planar probes, a 3D array was developed at the University of Utah (Campbell et al., 1991) and can now

be purchased from Cyberkinetics Inc. (<http://www.cyberkineticsinc.com/>). Beginning with a solid block of doped and conducting silicon, slices made with a micro-saw are cut most of the way through the block. Two subsequent etches produce a 3D, 10 \times 10 array of sharpened needles on a 4 \times 4 mm square. Metal and insulation layers are then applied to make a recording site on the tip of each shank with an interconnect running down the conducting silicon shank and through the back of the block, where gold pads are located for wire bonding to leads running to a skull-mounted connector. Each electrode is electrically isolated from neighboring electrodes by a moat of glass surrounding the base of each electrode. The 25–50 μm long recording tips are platinum or activated iridium, with impedances ranging from 50 to 500 k Ω and shank lengths ranging from 1.0 to 1.5 mm. The array is injected through the reflected dura with a special high-speed device to overcome the visco-elastic nature of the cortex, minimizing puckering during implantation. Leads are flexible, allowing the array to “float” on the cortical surface. This design has the advantage of placing a relatively large number of recording sites in a compact volume of cortex. Furthermore, recording sites at the tip are ideal in terms of sampling action potential fields and being located closest to the portion of cortex least damaged by insertion. However, with a single recording site at a fixed cortical depth, the Utah array suffers from the same fixed length problem as microwires. The large pyramidal cells in layer V are ideal for extracellular recording quality, as their potentials can be very large (300 microvolts in our experience) near their cell bodies, but the probe shanks are no longer than 1.5 mm, which is too short to reach those cell bodies. Probes of this length are also not good for recording in a sulcus, which is a problem in the motor cortex, where most of the area lies in the anterior bank of the central fissure. In the sulcus, the cortical layers are parallel to the electrode penetration so that the opportunity to record from many locations throughout layer V is lost with a single-length electrode (in contrast to a multisite shank).

Signal Processing. An effort is underway to build signal processing circuitry with telemetry onto chips that will be compatible with high-density silicon arrays (Ghovanloo and Najafi, 2004; Neihart and Harrison, 2005; Mohseni et al., 2005). On-chip telemetry eliminates the need for transcutaneous leads and a skull-mounted connector, removing a potential infection path, and greatly reduces the tethering forces generated by the dense bundle of output leads, allowing the device to float better.

Presently, BCI signal processing and computing is external, performed with large multiprocessing DSP platforms and PC controllers. However, several efforts are underway to dramatically miniaturize this technology and to reduce the power requirements so that complete systems can be implanted (Ji et al., 1991; Obeid et al., 2003, 2004). Generally, because of the high digital sampling rates (about 10 KHz) needed to capture the features of the spike waveform and the high channel count (around 100 per array), the sampling bandwidth is too high (about 1 MHz) to stream the recorded data continuously with a telemetry device. To address this problem, onboard spike sorting is being developed to isolate the unit waveform with the implanted device. This can be

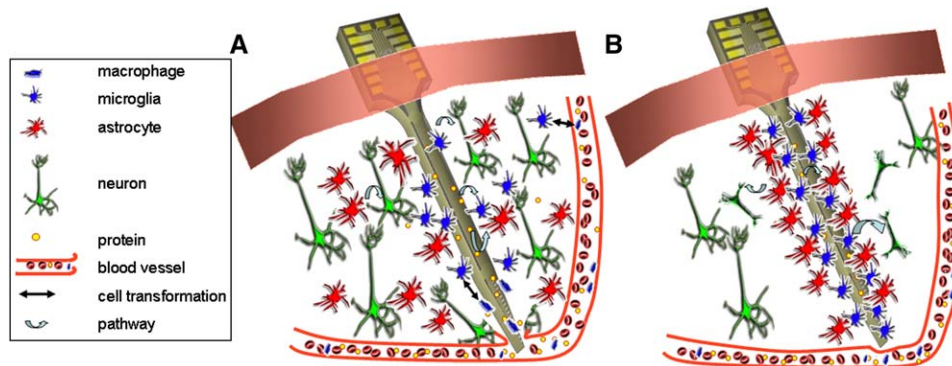


Figure 4. Cartoons Showing the Acute and Chronic Tissue Responses following Device Insertion

The acute response (A) is characterized by vasculature damage, neuronal injury, plasma protein adsorption, recruitment of activated microglia, and a broad region of reactive astrocyte around inserted devices. The chronic response (B) is characterized by a condensed sheath of cells primarily composed of activated microglia and reactive astrocytes around insertion sites. Degeneration of neuronal processes and additional neuronal loss may also be seen.

done by selectively transmitting one full bandwidth signal at a time, setting the sorting parameters externally, and back-transmitting the sorting parameters. Once the parameters are set on all channels, the transmitted data only consist of the time stamps indicating when each action potential occurred, greatly reducing the data flowing through the telemetry link.

Currently, spike data are processed by a real-time extraction algorithm on a separate processor, and the extracted signal is transmitted to the controlled device (e.g., computer graphics display or robot controller). Work is underway to downsize the processor platform so that it can be worn externally or contained within the prosthesis. Somatosensory approaches are now being explored that will provide mechanoreception of the generated movement using electrical stimulation to directly activate target populations of neurons in the sensory system (see below). This will require additional processing to transform the mechanical input to trains of stimuli, which will be transmitted to implanted electronics, which, in turn, generate the electrical stimulation.

Electrode-Tissue Interface

A critical, and possibly somewhat controversial, issue to be addressed in the BCI field is the interface between the electrode and the brain tissue in which it is embedded.

Although microfabricated neural electrode arrays have the ability to record high-quality signals, the majority have not demonstrated the long-term performance desired for prosthesis, i.e., stable recording over several years (Rousche and Normann, 1998; Liu et al., 1999; Williams et al., 1999b; Schwartz, 2004; Vetter et al., 2004). After implantation, the percentage of electrodes that record single-unit waveforms is low and drops over time. Recording quality varies both across subjects and even between electrode sites in the same array. The electrical, mechanical, and biochemical mismatch between implant and host tissue triggers CNS tissue responses, including neuronal loss and glial encapsulation, which may contribute to chronic recording failure.

Brain Tissue Response to Implanted Electrodes

For long-term stable recording, neuron-electrode proximity must be maintained. Neuronal density has been examined with immunohistology and shows a significant

loss around the implant (Edell et al., 1992; Biran et al., 2005). Putative reasons for this include the following: migration and micromotion of the implant; neuronal processes migrating away from the electrode; neuronal death due to insertion injury; or chronic inflammation and neuronal exclusion by the glial sheath. In contrast to the volume around the shank of the electrode, cell density appears normal near the tip, suggesting that recording sites located there may be advantageous.

Reactive tissue response to the implant has been categorized into two stages: acute response and chronic inflammation (Figure 4). Acute responses are triggered by device insertion and begin to subside after a week. This mechanical trauma initiates a CNS wound-healing response, including release of erythrocytes, clotting factors, and inflammatory factors from the disrupted blood vessels, which facilitates macrophage and microglia recruitment as well as astrocyte activation (Szarowski et al., 2003; Turner et al., 1999). This mechanically induced healing response is transitory; removal of the implant immediately after insertion leaves little evidence of tissue scarring after a 1 month recovery (Yuen and Agnew, 1995). However, sustained responses are maintained for a lifetime (Stensaas and Stensaas, 1976, 1978; Menei et al., 1994; Mofid et al., 1997; Emerich et al., 1999; Mokry et al., 2000; Szarowski et al., 2003). This chronic reaction is characterized by the presence of activated microglia at the implant surface, and a dense encapsulating layer of reactive astrocytes around the probe (Turner et al., 1999; Szarowski et al., 2003). The exact effect of reactive gliosis on chronic recording has not been clearly linked with histological and physiological studies, but it is hypothesized that encapsulation acts to insulate the electrode from nearby neurons and increase electrical impedance (Williams, 2001). An astrocytic scar may also direct neuronal processes away from “non-brain” structures, resulting in process retraction and signal strength deterioration (Reier et al., 1983; Edell et al., 1992). New data suggest that persistent macrophage activation may lead to chronic neuronal loss (Biran et al., 2005).

Conventionally, test animals are implanted with model probes and sacrificed at various time points to evaluate

the probe and adjacent neural tissue. Immunohistochemical staining is used to identify cell numbers, locations, types, and byproducts (Turner et al., 1999; Szarowski et al., 2003; Cui et al., 2003; Biran et al., 2005; Turner et al., 1999; Szarowski et al., 2003; Kim et al., 2004; Lin et al., 2005).

Histology cannot provide real-time information of the implant/tissue interface. Noninvasive, real-time methods using impedance spectroscopy can detect the degree of gliosis to some extent (Williams, 2001; Cui et al., 2003; Johnson et al., 2004) but lack sufficient resolution and biospecificity. MR-compatible silicon neural probes have been made as the first step (Santies-teban et al., 2006) in using high-resolution magnetic resonance imaging (MRI) to monitor electrode movement and the implant/tissue interface. Microdialysis has been proposed as a possible tool to sample the chemical environment near the implant site (Polikov et al., 2005). Immunosensors incorporated on the recording probe can monitor local cytokine levels and may provide real-time information on biochemical change at the very local level (Wadhwa and Cui, 2006).

Improving the Electrode-Tissue Interface. While efforts to improve implant design, electrode implantation, and securing techniques have shown effectiveness in obtaining more reliable and reasonably long-term recording (Suner et al., 2005), continued biomaterials and tissue engineering approaches are aimed at creating the ultimate probe-tissue interface. Surface texture has been considered an important factor for attachment and growth of various cell types. It has been shown that topographic features help promote the growth of neurites in vitro (Yuen and Agnew, 1995; James et al., 2000). A recent study demonstrated that nanoscale features, created by deposited nanotubes on a substrate surface, seem to encourage neuronal growth while inhibiting astrocyte attachment (Moxon et al., 2004a). Extracellular matrix (ECM) protein (collagen, laminin, fibronectin) or synthetic polymers containing ECM fragments have been deposited on the implant surface to promote neuronal growth (Mensingher et al., 2000; Buchko et al., 2000; Zhong et al., 2001; Cui et al., 2001, 2003; Cui and Martin, 2003; He and Bellamkonda, 2005) and better anchoring within the tissue (Buchko et al., 2000; Cui et al., 2001, 2003; Cui and Martin, 2003; He and Bellamkonda, 2005; Mensinger et al., 2000; Zhong et al., 2001). However, the ECM coatings are nonspecific, promoting ingrowth of all cell types, including those that compose the glial sheath, such as astroglia and meningeal fibroblasts. More neuron-specific molecules, such as neuron adhesion molecule L1, may be a better choice (Charley et al., 2005; Webb et al., 2001).

Another approach is to encourage neuronal ingrowth toward the implant by releasing neurotrophic factors. This has been demonstrated in a “neurotrophic electrode” design in which a piece of sciatic nerve was placed in a glass cone electrode before implantation. Cortical neurites grew into the cone, resulting in stable recordings for up to 15 months (Kennedy et al., 1992). Incorporation of nerve growth factor in hydrogel coating of neural probes has been tried in the CNS, but without positive results. The effectiveness of NGF is likely to be limited, since many CNS neurons are unresponsive

to this neurotrophin. However, other factors, such as BDNF, NT-3, and GDNF in CNS (Lu et al., 2005), may be potential candidates.

In addition to attracting neurons toward the electrode, a newly developed approach extends the recording site into the parenchyma. A conducting polymer has been demonstrated to be polymerizable in live tissue (Richardson-Burns et al., 2005). It grows from the electrode surface toward neurons, resulting in an intimate neuron-electrode connection. Questions remain as to how to control polymer growth without losing single-unit resolution and whether the neurons will tolerate contact with the synthetic polymer.

Use of anti-inflammatory drugs has also been investigated (Shain et al., 2003). Peripheral injections and local elution of Dexamethasone (Dex), a synthetic glucocorticoid that can reduce inflammation in the CNS, have been shown to effectively minimize reactive tissue response to neural implants in rats (Turner et al., 1999; Spataro et al., 2005; Meilander et al., 2001; Kim and Martin, 2006). Controlled release with a microfluidic-based system (Retterer et al., 2004) or with an electrical delivery system (Wadhwa et al., 2006) is being developed and may be more precise. However, confirmation of anti-inflammatory effectiveness in terms of recording enhancement has not been carried out.

Extraction Algorithms

The results of experiments performed by Georgopoulos and his colleagues in the 1980s showed that detailed movement information could be easily recognized in the activity patterns of motor cortical neurons, thus paving the way for the current generation of BCIs. Unlike previous experiments studying single joints, this work, carried out with monkeys trained to make arm movements in different directions, found that the intensity of recorded activity was related to movement direction in a simple, direct, and robust manner. Linear regression in two (Georgopoulos et al., 1982) and three (Schwartz et al., 1988) dimensions showed that these cells were cosine tuned to movement direction, and that this tuning function had a single “preferred direction” where the cell fires at a maximal rate. These preferred directions tend to be distributed uniformly. By representing each unit with a vector in its preferred direction, weighting the vector by each cell’s firing rate, and summing these contributions vectorially, the direction of upcoming arm movement can be extracted from the population (Georgopoulos et al., 1983). When this is done in small time intervals (10–40 ms), the resulting population vectors correspond to the upcoming velocity of the moving arm (Georgopoulos et al., 1986). This principle—simple linear extraction of movement kinematics—is the basis for almost all current real-time extraction algorithms. Enhancements using linear and nonlinear filters and pattern recognition algorithms are being developed and promise to be more efficient (better prediction with fewer units) than current algorithms. Most of the power from these techniques will likely come from the use of a more elaborate state space model of movement. For instance, most movements are smooth, with minimal jerk, and faster movements tend to be straight. Modeling this information will limit the range of possible predictions made by the extraction algorithm. The

combination of these algorithms with new insights into how subjects learn to modify their neural activity when using these devices (see below) is a current research thrust that will become increasingly important as these devices are used for more demanding movements including those of the hand and finger.

New techniques for deriving movement-control signals from populations of recorded cortical activity are being developed rapidly (Brown et al., 2004; Kass et al., 2005). Extraction algorithms can be categorized broadly into inferential methods and classifiers (Schwartz et al., 2001; Schwartz, 2004). Empirically derived models are the basis for inferential methods and include the population vector (see above), optimal estimators (Salinas and Abbott, 1994), and linear (Paninski et al., 2004; Wu et al., 2004; Wu et al., 2006) and nonlinear (Brockwell et al., 2004; Rojas et al., 2005) filters. Classifiers require no basic understanding of the relation between neural activity and behavior, relying instead on consistent patterns within and between variables (Fetz, 1999) and include self-organizing feature maps (Lin et al., 1997), back-propagation (Wessberg et al., 2000), and maximum-likelihood methods (Pouget et al., 1998; Schwartz et al., 2001; Kemere et al., 2004).

Filter techniques take into account the current and historic state of the ongoing movement, using motor variables that vary in a regular and predictable way. During the time-varying process underlying a motor act, this state model is combined with instantaneous neural activity to update the predicted (intended) movement. Development of more sophisticated state space models will likely enhance cortical prosthetic control (see above). Another important factor in the success of any extraction method is how well the subject can learn to use the algorithm. It may turn out that a simple approach, using, for instance, the population vector algorithm, may be just as, or more, powerful than more elaborate approaches. The demonstrated learning that takes place with these algorithms in closed-loop algorithms is responsible for an increased performance with fewer recorded units (Taylor et al., 2002; Lebedev et al., 2005; Kim et al., 2006).

Learning, manifest as feedback-dependent changes in neural activity, serves an important role in achieving high performance with brain-controlled interfaces. So far, the feedback signal has only been visual—for instance, a monkey may watch a computer display or robot arm and make online corrections to the movement or improve the cosine fit of the neural activity recorded with the chronic electrodes. Again, as prosthetic complexity increases, somatosensory input will become more important.

Somatosensation

Somatosensory feedback is a vital component of motor planning, control, and adaptation, and there is a growing effort to include this feedback in neural prosthetic systems. In the intact neuromuscular system, information about the physical state of the limb is transduced and carried by primary afferent neurons, consisting of several types of cells, including muscle spindles, golgi tendon organs, and joint and cutaneous receptors. Fibers from these cells project to the spinal cord, where they branch to form local and ascending projections onto neurons in the dorsal horn and brainstem, respectively. The incoming somatosensory information undergoes

further synaptic processing in the thalamus before arriving in sensory cortex.

Two general classes of somatosensory neural interfaces (SSNI) are being developed for neural prosthetic systems, and we refer to these as Sensory Input or Sensory Output to indicate the direction of information flow across the neural interface. The Sensory Output class uses measurements of afferent neural activity to derive state feedback, for example, to control functional electrical stimulation (FES) systems (Haugland and Sinkjaer, 1999; Strange and Hoffer, 1999). Conversely, a Sensory Input neural interface is used to transmit information into the nervous system. A highly successful example is the cochlear implant (CI), a device that restores auditory sensations by converting sound into electrical stimuli applied to the auditory nerve (Rubinstein, 2004). Although the CI has achieved widespread clinical success for the hearing impaired, an analogous device for somatosensation has not been developed for those in need of motor prosthetics.

Sensory Recording Interfaces

Loeb was the first to suggest that neural recordings from intact cutaneous and proprioceptive afferents could be used to provide sensory feedback for controlling FES systems (Loeb et al., 1977). Two separate groups, headed by Loeb and Prochazka (Prochazka et al., 1976), pioneered the development of somatosensory neural recording interfaces 30 years ago. Both used microwires implanted chronically in the dorsal roots or dorsal root ganglia (DRG) to record simultaneously from multiple primary afferent neurons in awake, behaving cats. More recently, Stein and colleagues have started using Utah electrode arrays to record simultaneously from more than 100 neurons in the L6 and L7 of the cat DRG (Stein et al., 2004). Figure 5 shows a diagram of a microelectrode array implanted in the DRG. A subset of units with high correlation to kinematic variables can be selected and used to decode limb position and velocity variables from the ensemble of afferent firing rates in both anesthetized (Stein et al., 2004) and awake, walking cats (Weber et al., 2006). Multichannel afferent recordings have also been obtained during FES-evoked hindlimb stepping in an anesthetized cat (Figure 5). The afferent activity recorded during FES can be decoded to estimate limb kinematics with a high degree of accuracy and could provide valuable feedback for an FES controller.

Another method for recording afferent neural activity is to use a nerve cuff, an insulating sleeve containing multiple electrodes for recording action currents flowing along its interior length (Stein et al., 1975). Unlike microelectrodes, which can record selectively from single neurons, electroneurograms (ENGs) recorded by the nerve cuff represent the combined activity of all nerve fibers passing through the cuff. Nevertheless, useful information can be derived from nerve cuff recordings, and multiple types of closed-loop FES control systems have been developed with feedback derived from cuff signals. For example, Haugland and Sinkjaer (1999) created two different human FES systems, one for correcting foot drop and the other for restoring hand grasp, using cuff recordings from cutaneous nerves to provide ground contact or grasp force feedback, respectively.

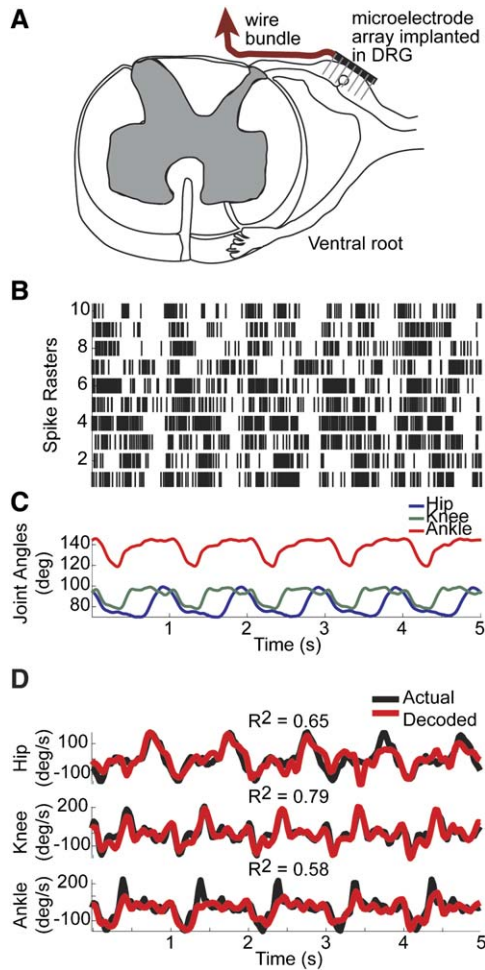


Figure 5. Sensory Extraction

(A) An array of penetrating microelectrodes is inserted into the DRG to record simultaneously from several primary afferent neurons. (B) Rasters of spike activity from ten primary afferent neurons during FES-evoked hindlimb stepping. (C) The corresponding hip, knee, and ankle joint angles. (D) Joint angular velocities were decoded from the ensemble of afferent firing rates. These data were recorded in the laboratory of Dr. Richard Stein at the University of Alberta in collaboration with one of the authors (D.J.W.).

The nerve cuff electrode has also been used as a bidirectional interface, enabling both recording of afferent ENG signals and stimulation of motor axons in peripheral nerves. Hoffer (Hoffer et al., 2005) has developed and commercialized Neurostep™, a closed-loop controlled FES system for patients with foot drop. This device is a fully implanted system consisting of a stimulator control unit implanted in the thigh and nerve cuff electrodes placed on the common peroneal and tibial nerves. Heel contact and toe lift events are identified in the ENG signals and used to control the timing of electrical stimulation during walking.

In summary, it is clear that primary afferent neurons are a rich source of body state information that could provide useful feedback for controlling a neural prosthesis. Thus far, the only sensory feedback-controlled FES systems to be tested in humans have used nerve cuff electrodes. Multiple single-unit recordings with micro-

electrode arrays implanted in the DRG (Weber et al., 2006) or spinal cord (Borisoff et al., 2006) may provide more information than cuff recordings, but the long-term reliability of these approaches remains to be proven.

Sensory Input Interfaces

The function of a somatosensory neural input interface is to transmit the physical state of the prosthetic limb to the neural networks supporting perception and feedback control in the CNS. Generally, approaches to sensory neuroprostheses fall into one of two categories: substitution or replacement. Sensory substitution systems “display” sensory information through a sensory channel (eye, ear, or skin) that is different from that normally used (Kaczmarek et al., 1991). In contrast, sensory replacement engages, as much as possible, the neural pathways normally involved in sensory reception and processing.

To communicate the full range of sensory modalities for an entire limb, it will be necessary to stimulate large numbers of neurons in parallel. Multichannel microstimulation methods are being tested using microelectrode arrays implanted at various locations along the somatosensory neuraxis, from peripheral nerves to primary sensory cortex. An important goal of current research in this area is to determine the optimal location and electrode design for creating a somatosensory neural stimulation interface. Factors to consider in this assessment include the mechanical stability of the implant site, tissue response to chronic implantation, the number of channels needed, the clarity of the evoked perceptual responses, and the generation of undesirable side effects such as pain or seizures.

Tactile (Torebjork et al., 1987) and proprioceptive (Dhillon et al., 2004) sensation are naturally transmitted through primary afferents to the somatosensory nervous system, and electrical stimulation of these neurons can evoke the same sensation (Vallbo, 1981; Dhillon et al., 2004). Several types of implantable electrodes have been developed to stimulate directly the remaining portions of severed axons. The regeneration electrode was designed to take advantage of the regrowing peripheral nerves by encouraging axonal sprouting through holes in an electrode grid (Mannard et al., 1974; Stein et al., 1975; Kovacs et al., 1992; Dario et al., 1998). Longitudinal Intrafascicular Electrodes (LIFE) were designed for insertion into a nerve bundle to record or electrically stimulate adjacent nerve fascicles (Malagodi et al., 1989), and Yoshida et al. (Yoshida and Horch, 1993) showed that LIFE electrodes can selectively activate subpopulations of axons within a single fascicle. Recently, Dhillon et al. (Dhillon et al., 2004; Dhillon and Horch, 2005) used LIFE electrodes to stimulate afferents in the peripheral nerve stump of long-term amputees and were able to evoke discriminable sensations of touch, joint movement, and position. They also found an amplitude (1–200 μ A)- and frequency (<1 kHz)-dependent effect, suggesting its usefulness for graded or proportional sensation.

The findings of Dhillon et al. (Dhillon et al., 2004; Dhillon and Horch, 2005) show that (1) primary afferent neurons remain viable in long-term amputees and can support a sensory neural interface, and (2) electrical stimulation of primary afferent neurons can produce

conscious, discriminable, and proportional sensation of touch and proprioception. Although encouraging, more work is needed to develop a somatosensory neural interface that is mechanically and electrically stable and can transmit enough information to describe the full state of the limb.

Several groups are currently testing microstimulation methods in somatosensory regions of the brain, such as the thalamus and primary sensory cortex, although no reports have been published as of this writing. For evoking tactile sensations, it is clear from the work of Romo and colleagues (Romo et al., 2000) that intracortical microstimulation can evoke discriminable, graded perceptions of flutter stimuli. Intraneural microstimulation studies in humans have also shown that stimulation of single cutaneous afferents evokes conscious, frequency-dependent illusions of flutter or vibration (Macefield, 2005). Although two-choice discrimination tasks can be learned with microstimulation, it is unclear whether more complex and dynamic tactile or proprioceptive perceptions can be conveyed with this or any other approach.

Effectors

Once a control signal has been extracted, it is fed to an external device to effect movement. This motion ranges from cursors moving on a computer display to the operation of anthropomorphic robot arms. The general scheme is to sample the neural data continuously and then at some interval, for example 30 ms, to generate a control signal update from this activity. This differs from classical systems neurophysiology approaches, as this must be done in real time without any trial averaging.

Moving a cursor on a computer display with this approach is straightforward, since the control signal is usually in a kinematic (i.e., X-Y) coordinate frame that can be mapped easily to computer displays. In contrast, the transformation needed for robot control is more difficult, although some robot controllers have built-in inverse kinematic software that translates an endpoint coordinate to a series of motor rotations. However, to accomplish anthropomorphic joint rotations, another layer of complexity is needed, since an anthropomorphic arm has more degrees of freedom than endpoint coordinate axes. For the elbow and shoulder joints, good performance can be obtained with a relatively simple procedure (Soechting and Ross, 1984; Kang et al., 2005). However, an equivalent framework for the much larger complexity of the wrist, hand, and fingers is unknown.

FES, a method of applied electrical stimulation to contract muscles, holds the promise of “reanimating” paralyzed limbs (Loeb and Davoodi, 2005). This approach can be enhanced by using cortical activity as a control source, since these signals contain many of the natural features of intended movement (Schwartz and Moran, 2000). Conventional cortical signals used for brain-controlled signals are in the form of position and velocity of the endpoint (hand or cursor). To generate muscle contractions to move the arm in this coordinate frame with this control signal, inverse kinematics must be performed with an ordered set of operations. First, a combination of joint displacements must be selected, then the

torques needed to generate these displacements calculated. To produce these torques, a set of muscles must be selected and their contractile forces specified. Finally, a set of muscle activations must be computed to generate the desired muscle force. Since there are many muscle combinations that can be used to generate a given joint torque, and many joint displacements that can be used for a specific endpoint shift, choices must be made for each of these steps. However, once made, these choices result in a deterministic displacement. Contrary to intuition, the reverse operation of using forward dynamics to calculate endpoint movement is not as robust. Attempts are underway to intercept motor signals in peripheral nerves or to consider cortical output in terms of muscle activation as a more “direct” way to specify movement. While in principle this should work, this approach is fraught with a number of serious practical difficulties. First is a sampling problem; if some of the motor signals are missed, the entire solution at the end of two integrative steps can be quite erroneous. There is also the issue of transforming the muscle activation signal to muscle force, which requires a nonlinear solution dependent on muscle length and velocity. To get joint torques, an accurate musculoskeletal model is needed, with accurate bone-muscle geometries and mass distributions. The final step to get displacement requires that all forces, including torques, interactive forces (from other moving skeletal segments), and external forces (such as gravity and applied loads), be summed correctly (Hollerbach and Flash, 1982; Soechting, 1983). Since this entire procedure is done step by step as an integration, small errors tend to propagate and expand. Although many of the same requirements are needed for both the reverse and forward schemes, the desired endpoint is “known” for each step of the inverse kinematic process, obviating the integrative errors so problematic with the opposite approach. This is a current topic of interest with demonstrated use in relatively simple, stereotypic movement (Grill and Peckham, 1998; Crago et al., 1998; Lauer et al., 1999; Kirsch et al., 2001; Peckham et al., 2002; Kurosawa et al., 2005; Bogey et al., 2005; Kuiken, 2006).

BCI Progress

An early demonstration of intracortical signals harnessed to a machine used a rat with microwires implanted in its motor cortex (Chapin et al., 1999). The recorded signals were processed and used to move a water drop on a lever toward the animal’s mouth. Soon after, it was shown that 3D arm trajectories could be extracted from single trials of recorded population activity (Isaacs et al., 2000). In this task, a rhesus monkey used its arm to reach from the center to the corners of a cube while activity from a population of more than 30 neurons was recorded simultaneously with microwires. A pattern-matching algorithm was used to construct neural trajectories that closely matched the actual 3D trajectories. An open-loop paradigm in which the movement generated from the recorded activity was not displayed back to the animal was also used in a subsequent report (Wessberg et al., 2000). The open-loop distinction is important here because the animals had no knowledge of the brain-derived signal being used for predicting arm trajectory and could not modify the

recorded neural activity to improve the prediction. In these subsequent experiments, owl monkeys performed one-dimensional movements by pulling a lever. The animals monitored the lever movement on a computer display while populations of cortical activity were recorded. This activity was processed in real time with an extraction algorithm based on linear multiple regression and the processed output used to control a robot arm. In a second task, the monkey reached in 3D space in a self-feeding task. Predicted trajectories were generated from recorded activity, and some of these were also used to control the (unseen) robot arm.

The control loop was closed by having monkeys view cursor movements controlled directly by cortical activity (Taylor et al., 2002; Serruya et al., 2002). In the Taylor et al. work, monkeys initially reached from the center of a cube (displayed in a stereo monitor) to each of its corners so that a 3D tuning function of each chronically recorded unit could be calculated. The animals' arms were then restrained and population vectors processed from the recorded activity as each target was again presented. A new population vector was generated at 30 ms intervals and used to update the position of the cursor in the 3D display. The monkeys rapidly learned to move the cursor to the corner targets in this condition. Interestingly, it was found that the preferred directions of the recorded cells would rotate once an animal's arms were restrained. To account for this, a coadaptive algorithm tracked changes in each cell's preferred direction during the daily recorded sessions as the task progressed. With this approach, the monkeys achieved high performance, moving a brain-controlled cursor swiftly and accurately to a variety of 3D targets. Their performance was robust, as they could carry out the task with a greater than 90% success rate for an hour at a time over multiple days. With practice, firing rates during brain-controlled movements fit the cosine tuning function better—the firing rate variance accounted for by the regression equation increased over days, and this was partially responsible for the increased performance. Displaying the derived movement makes it possible for the subject to modify the recorded activity patterns to achieve a more desired movement. These closed-loop learning approaches will be an important aspect of future prosthetic applications.

In addition to the virtual movement displays on computer monitors, it is necessary to demonstrate the efficacy of physical brain-controlled devices. This establishes that subjects have the real-world ability to overcome noisy actuators operating in a physical environment. Furthermore, physical interaction can potentially enhance the “embodiment” of the device so that it feels that the prosthesis has been incorporated. This is a topic of current interest in both psychology and artificial intelligence, where embodiment is considered to be an important component in the development of cognition and intelligence (Edelman, 1985; Brooks, 1991).

The first report of a brain-controlled, anthropomorphic robot arm appeared in 2003 (Taylor et al., 2003). In this report, monkeys first were trained to use brain control to move to targets in 3D space as in Taylor et al. (2002). After achieving high performance in this task, the brain-derived control signal was shifted from the computer cursor to the robot controller. Now the

cursor in the display represented the position of the robot's wrist in 3D space but looked the same to the monkey, even though the cursor was now coupled to the noisy movement of the robot arm. This arm had inertia, stiction, and general control errors. The suboptimal mechanical performance of the arm appeared as perturbations of cursor movement, which the monkey was able to overcome, achieving a performance near that of the ideal cursor movement in the VR task. Subsequently, another report based on a similar indirect visualization paradigm (Carmena et al., 2003) used planar robot movements with a gripper at the end of a robot arm. Here too, the animal saw the task on a computer monitor without directly viewing the arm. The aperture of the gripper was specified as circles of different radii to be matched by cursors of the same size. In current work (M. Spalding et al., 2005, Soc. Neurosci., abstract; M. Spalding et al., 2004, Soc. Neurosci., abstract), monkeys view the robot arm directly during 3D brain control. This anthropomorphic arm's shoulder is suspended near the monkey's own shoulder. Both of the animal's own arms are restrained. A motorized gripper at the end of the arm opens with movement away from the animal and closes when leaving the target. Targets are food pieces held out by an investigator to be grasped and retrieved to the animal's mouth. The velocity signal derived from the population vector algorithm corresponds to the robot endpoint (grripper), so an inverse kinematic calculation is used to derive the joint angles at each time step of the task. In this paradigm, the tuning functions of the recorded unit were found in the absence of movement with an iterative method (Wahnoun et al., 2006). Food targets were initially presented in four locations in front of the animal, and the directions from the gripper's initial position to each target and back to the mouth were used in the initial calculation of the tuning function. It was assumed that the animal was initially attempting to reach the food and that the neural activity would be modulated appropriately. To complete the task, the arm moved automatically to the targets after a preset interval. This was repeated iteratively until the tuning function estimates stabilized.

Intracranial Human Studies

Brain-controlled interfaces are generally divided into the categories of invasive and noninvasive, as described in “Recording Technology” above. Although it is commonly assumed that the invasive approach is more dangerous, this may not be the case, especially with the new telemetric devices under development. Intracortical electrodes will penetrate only the outer 2–3 mm of cortex and have a footprint of less than a square cm. Recent reports of deep brain stimulation implants show that the infection rate attributable to the surgical procedure is 1.5%–2%, while the long-term infection rate is about 4%–5% (Voges et al., 2006; Deuschl et al., 2006). It can be assumed that the 1%–2% infection rate is going to be representative of the cortical implants with telemetry, since they will be smaller and more superficial than DBS devices. At this point, it seems likely that implantation of chronic cortical electrodes will be relatively safe.

Two teams have implanted intracranial electrodes in human motor cortex for prosthetic control. Kennedy and colleagues (Kennedy et al., 2000, 2004) have implanted several paralyzed patients with the neurotrophic

cone electrode (see above) and a telemetry device contained beneath the scalp. The electrode recorded action potentials and LFPs for extended periods of time. These patients, who were completely immobilized, were able to modulate the recorded signals, and at least one of them learned to communicate with a simple speller routine on a computer display.

Recently, Hochberg et al. (2006) reported results of a human quadriplegic implanted with a Utah array. Over a 9 month period, the patient performed a number of tasks with the "BrainGate" device. He learned to use the recorded signals to move a cursor on a 2D computer screen, and it was reported that he was able to open and close a robotic hand. Furthermore, he "used a simple multi-jointed robotic limb to grasp an object and transport it . . ." The cursor movements were in general ataxic, with "underlying instabilities and variable oscillatory components" and an inability to stabilize the cursor, while the hand movement was a binary open/close motion. The robot arm was moved in only a single direction when the subject touched (with great difficulty) the computer cursor to one of four targets. This initial performance was poorer than the 3D movements generated by nonhuman primate studies (Taylor et al., 2002) and may be related to the extraction algorithm used and/or the quality of the neural recordings. The array length used in this first implant was only 1 mm, too short to reach the cell bodies of the large pyramidal cells in layer V of motor cortex. Their most recent patient (Donoghue and Hochberg, 2006) had significantly better neural recordings with a longer array (1.5 mm) and was able to stabilize the cursor with an improved extraction algorithm, suggesting that further technological improvements hold promise for better performance. These human studies show that patients are capable of volitionally modulating motor cortical activity even after prolonged immobility. They have also shown that chronic recordings are feasible and that additional development will lead to improved performance.

Conclusion

Whether brain-controlled interfaces gain widespread use among the patient population will depend on a number of factors. These include performance, perceived and actual safety, cost, and improvement in quality of life. Performance at this time is most severely constrained by the ability of our chronic electrodes to record robust single units for long durations. A secondary aspect is how well new extraction algorithms will perform as more complex parameter sets are needed for elaborate movements. Safety of these implanted devices will be enhanced as integrated low-power electronics and telemetry eliminate transcutaneous connectors. Cost may be affected by our ability to utilize techniques developed in the microfabrication industry and in their commercialization applied to prosthetic devices. Finally, quality of life enhancement will depend on the patient's deficit. Locked-in patients will benefit from any technology that allows them even a simple communication channel. In contrast, people with C5-C6 spinal cord lesions have residual arm movement and will only benefit from a prosthesis that adds enhanced wrist and hand movement. Few patients have the more severe deficits, so that the popularity of future devices will increase only

when they can provide coordinated movement that is relatively complex, sophisticated, and agile. The rapid development, current demonstrations, and ensuing excitement in the field of neural prosthetics suggest that this will happen soon.

Acknowledgments

This work was supported by NIH NINDS (A.B.S.) and DARPA (A.B.S. and D.J.W.), a Wallace Coulter Foundation Translational Research Early Career Award (X.T.C.), the University of Pittsburgh Competitive Medical Research Fund (X.T.C.), the Central Research Development Fund (X.T.C.), the Whitaker Foundation (D.W.M.), and the Hartwell Foundation (D.W.M.).

References

- Andersen, R.A., Musallam, S., and Pesaran, B. (2004). Selecting the signals for a brain-machine interface. *Curr. Opin. Neurobiol.* 14, 720–726.
- Biran, R., Martin, D.C., and Tresco, P.A. (2005). Neuronal cell loss accompanies the brain tissue response to chronically implanted silicon microelectrode arrays. *Exp. Neurol.* 195, 115–126.
- Birbaumer, N., Ghanayim, N., Hinterberger, T., Iversen, I., Kotchoubey, B., Kubler, A., Perelmouter, J., Taub, E., and Flor, H. (1999). A spelling device for the paralysed. *Nature* 398, 297–298.
- Bogey, R.A., Perry, J., and Gitter, A.J. (2005). An EMG-to-force processing approach for determining ankle muscle forces during normal human gait. *IEEE Trans. Neural Syst. Rehabil. Eng.* 13, 302–310.
- Borisoff, J.F., McPhail, L.T., Saunders, J.T., Birch, G.E., and Ramer, M.S. (2006). Detection and classification of sensory information from acute spinal cord recordings. *IEEE Trans. Biomed. Eng.* 53, 1715–1719.
- Brockwell, A.E., Rojas, A.L., and Kass, R.E. (2004). Recursive bayesian decoding of motor cortical signals by particle filtering. *J. Neurophysiol.* 91, 1899–1907.
- Brooks, R.A. (1991). Intelligence without representation. *Artificial Intelligence Journal* 47, 139–159.
- Brown, E.N., Kass, R.E., and Mitra, P.P. (2004). Multiple neural spike train data analysis: State-of-the-art and future challenges. *Nat. Neurosci.* 7, 456–461.
- Buchko, C.J., Slattery, M.J., Kozloff, K.M., and Martin, D.C. (2000). Mechanical properties of biocompatible protein polymer thin films. *J. Mater. Res.* 15, 231–242.
- Buzsaki, G., and Kandel, A. (1998). Somadendritic backpropagation of action potentials in cortical pyramidal cells of the awake rat. *J. Neurophysiol.* 79, 1587–1591.
- Campbell, P.K., Jones, K.E., Huber, R.J., Horch, K.W., and Normann, R.A. (1991). A silicon-based, three-dimensional neural interface: Manufacturing processes for an intracortical electrode array. *IEEE Trans. Biomed. Eng.* 38, 758–768.
- Carmena, J.M., Lebedev, M.A., Crist, R.E., O'Doherty, J.E., Santucci, D.M., Dimitrov, D.F., Patil, P.G., Henriquez, C.S., and Nicolelis, M.A.L. (2003). Learning to control a brain-machine interface for reaching and grasping by primates. *PLOS Biol.* 7, E42. Published online October 13, 2003. 10.1371/journal.pbio.0000042.
- Chapin, J.K., Moxon, K.A., Markowitz, R.S., and Nicolelis, M.A. (1999). Real-time control of a robot arm using simultaneously recorded neurons in the motor cortex. *Nat. Neurosci.* 2, 583–584.
- Charley, E.A., Lagenaur, C.F., Stauffer, W.R., and Cui, X. (2005). Improving brain tissue integration of the neural probes through surface immobilization of biomolecules. *Regenerate*, Atlanta, GA.
- Cooper, R., Winter, A.L., Crow, H.J., and Walter, W.G. (1965). Comparison of subcortical, cortical and scalp activity using chronically indwelling electrodes in man. *Electroencephalogr. Clin. Neurophysiol.* 18, 217–228.
- Crago, P.E., Memberg, W.D., Usey, M.K., Keith, M.W., Kirsch, R.F., Chapman, G.J., Katorgi, M.A., and Perreault, E.J. (1998). An elbow extension neuroprosthesis for individuals with tetraplegia. *IEEE Trans. Rehabil. Eng.* 6, 1–6.

- Cui, X., and Martin, D.C. (2003). Electrochemical deposition and characterization of poly(3,4-ethylenedioxythiophene) on neural microelectrode arrays. *Sens. Actuators B Chem.* 89, 92–102.
- Cui, X., Lee, V.A., Raphael, Y., Wiler, J.A., Hetke, J.F., Anderson, D.J., and Martin, D.C. (2001). Surface modification of neural recording electrodes with conducting polymer/biomolecule blends. *J. Biomed. Mater. Res.* 56, 261–272.
- Cui, X., Wiler, J., Dzaman, M., Altschuler, R.A., and Martin, D.C. (2003). In vivo studies of polypyrrole/peptide coated neural probes. *Biomaterials* 24, 777–787.
- Dario, P., Garzella, P., Toro, M., Micera, S., Alavi, M., Meyer, U., Valderrama, E., Sebastiani, L., Ghelarducci, B., Mazzoni, C., and Pastacaldi, P. (1998). Neural interfaces for regenerated nerve stimulation and recording. *IEEE Trans. Rehabil. Eng.* 6, 353–363.
- Deuschl, G., Schade-Brittinger, C., Krack, P., Volkmann, J., Schafer, H., Botzel, K., Daniels, C., Deutschlander, A., Dillmann, U., Eisner, W., et al. (2006). A randomized trial of deep-brain stimulation for Parkinson's disease. *N. Engl. J. Med.* 355, 896–908.
- Dhillon, G.S., and Horch, K.W. (2005). Direct neural sensory feedback and control of a prosthetic arm. *IEEE Trans. Neural Syst. Rehabil. Eng.* 13, 468–472.
- Dhillon, G.S., Lawrence, S.M., Hutchinson, D.T., and Horch, K.W. (2004). Residual function in peripheral nerve stumps of amputees: Implications for neural control of artificial limbs. *J. Hand Surg. [Am.]* 29, 605–615.
- Donchin, E., and Smith, D.B. (1970). The contingent negative variation and the late positive wave of the average evoked potential. *Electroencephalogr. Clin. Neurophysiol.* 29, 201–203.
- Donchin, E., Spencer, K.M., and Wijesinghe, R. (2000). The mental prosthesis: Assessing the speed of a P300-based brain-computer interface. *IEEE Trans. Rehabil. Eng.* 8, 174–179.
- Donoghue, J.P., and Hochberg, L.R. (2006). Special report: BrainGate trial update: Spinal cord injury, stroke and ALS. *Neural Interfaces Workshop*, August 21, 2006, Bethesda, MD.
- Donoghue, J.P., Sanes, J.N., Hatsopoulos, N.G., and Gaal, G. (1998). Neural discharge and local field potential oscillations in primate motor cortex during voluntary movements. *J. Neurophysiol.* 79, 159–173.
- Ebersole, J.S. (1997). Defining epileptogenic foci: Past, present, future. *J. Clin. Neurophysiol.* 14, 470–483.
- Edell, D.J., Toi, V.V., Mcneil, V.M., and Clark, L.D. (1992). Factors influencing the biocompatibility of insertable silicon microshafts in cerebral cortex. *IEEE Trans. Biomed. Eng.* 39, 635–643.
- Edelman, G.E. (1985). Neural Darwinism: Population thinking and higher brain function. In *How We Know* (Nobel Conference XX), M. Shafiq, ed. (San Francisco: Harper & Row), pp. 1–30.
- Elbert, T., Rockstroh, B., Lutzenberger, W., and Birbaumer, N. (1980). Biofeedback of slow cortical potentials. I. *Electroencephalogr. Clin. Neurophysiol.* 48, 293–301.
- Emerich, D.F., Tracy, M.A., Ward, K.L., Figueiredo, M., Qian, R.L., Henschel, C., and Bartus, R.T. (1999). Biocompatibility of poly (DL-lactide-co-glycolide) microspheres implanted into the brain. *Cell Transplant.* 8, 47–58.
- Fetz, E.E. (1999). Real-time control of a robotic arm by neuronal ensembles. *Nat. Neurosci.* 2, 583–584.
- Freeman, W.J., Holmes, M.D., Burke, B.C., and Vanhatalo, S. (2003). Spatial spectra of scalp EEG and EMG from awake humans. *Clin. Neurophysiol.* 114, 1053–1068.
- Georgopoulos, A.P., Kalaska, J.F., Caminiti, R., and Massey, J.T. (1982). On the relations between the direction of two-dimensional arm movements and cell discharge in primate motor cortex. *J. Neurosci.* 2, 1527–1537.
- Georgopoulos, A.P., Caminiti, R., Kalaska, J.F., and Massey, J.T. (1983). Spatial coding of movement: A hypothesis concerning the coding of movement direction by motor cortical populations. *Exp. Brain Res. (Suppl. 7)*, 327–336.
- Georgopoulos, A.P., Schwartz, A.B., and Kettner, R.E. (1986). Neuronal population coding of movement direction. *Science* 233, 1357–1440.
- Georgopoulos, A.P., Langheim, F.J., Leuthold, A.C., and Merkle, A.N. (2005). Magnetoencephalographic signals predict movement trajectory in space. *Exp. Brain Res.* 167, 132–135.
- Ghovanloo, M., and Najafi, K. (2004). A modular 32-site wireless neural stimulation microsystem. *IEEE J. Solid-State Circ.* 39, 2457–2466.
- Grill, J.H., and Peckham, P.H. (1998). Functional neuromuscular stimulation for combined control of elbow extension and hand grasp in C5 and C6 quadriplegics. *IEEE Trans. Rehabil. Eng.* 6, 190–199.
- Haugland, M., and Sinkjaer, T. (1999). Interfacing the body's own sensing receptors into neural prosthesis devices. *Technol. Health Care* 7, 393–399.
- He, W., and Bellamkonda, R.V. (2005). Nanoscale neuro-integrative coatings for neural implants. *Biomaterials* 26, 2983–2990.
- Heldman, D.A., Wang, W., Chan, S.S., and Moran, D.W. (2004). Local field potential spectral tuning in primary motor cortex. San Diego, CA.
- Heldman, D.A., Wang, W., Chan, S.S., and Moran, D.W. (2006). Local field potential spectral tuning in motor cortex during reaching. *IEEE Trans. Neural Syst. Rehabil. Eng.* 14, 180–183.
- Henze, D.A., Borhegyi, Z., Csicsvari, J., Mamiya, A., Harris, K.D., and Buzsaki, G. (2000). Intracellular features predicted by extracellular recordings in the hippocampus in vivo. *J. Neurophysiol.* 84, 390–400.
- Hochberg, L.R., Serruya, M.D., Friehs, G.M., Mukand, J.A., Saleh, M., Caplan, A.H., Branner, A., Chen, D., Penn, R.D., and Donoghue, J.P. (2006). Neuronal ensemble control of prosthetic devices by a human with tetraplegia. *Nature* 442, 164–171.
- Hoffer, J.A., Baru, M., Bedard, S., Calderon, E., Desmoulin, G., Dhanwan, P., Jenne, G., Kerr, J., Whittaker, M., and Zwimpfer, T.J. (2005). Initial results with fully implanted Neurostep FES system for foot drop. Montreal, Quebec, Canada.
- Hollerbach, J.M., and Flash, T. (1982). Dynamic interactions between limb segments during planar arm movement. *Biol. Cybern.* 44, 67–77.
- Isaacs, R.E., Weber, D.J., and Schwartz, A.B. (2000). Work toward real-time control of a cortical neural prosthesis. *IEEE Trans. Rehabil. Eng.* 8, 196–198.
- James, C.D., Davis, R., Meyer, M., Turner, A., Turner, S., Withers, G., Kam, L., Banker, G., Craighead, H., Isaacson, M., et al. (2000). Aligned microcontact printing of micrometer-scale poly-L-lysine structures for controlled growth of cultured neurons on planar microelectrode arrays. *IEEE Trans. Biomed. Eng.* 47, 17–21.
- Ji, J., Najafi, K., and Wise, K.D. (1991). A low-noise demultiplexing system for active multichannel microelectrode arrays. *IEEE Trans. Biomed. Eng.* 38, 75–81.
- Johnson, M.D., Otto, K.J., Williams, J.C., and Kipke, D.R. (2004). Bias voltages at microelectrodes change neural interface properties in vivo. *Proceedings of the 26th International Conference of the IEEE-EMBS* 4103–4106.
- Kaczmarek, K.A., Webster, J.G., Bach-y-Rita, P., and Tompkins, W.J. (1991). Electrotactile and vibrotactile displays for sensory substitution systems. *IEEE Trans. Biomed. Eng.* 38, 1–16.
- Kang, T., He, J., and Tillery, S.I. (2005). Determining natural arm configuration along a reaching trajectory. *Exp. Brain Res.* 167, 352–361.
- Kass, R.E., Ventura, V., and Brown, E.N. (2005). Statistical issues in the analysis of neuronal data. *J. Neurophysiol.* 94, 8–25.
- Kemere, C., Shenoy, K.V., and Meng, T.H. (2004). Model-based neural decoding of reaching movements: A maximum likelihood approach. *IEEE Trans. Biomed. Eng.* 51, 925–932.
- Kennedy, P.R., Mirra, S.S., and Bakay, R.A.E. (1992). The cone electrode—Ultrastructural studies following long-term recording in rat and monkey cortex. *Neurosci. Lett.* 142, 89–94.
- Kennedy, P.R., Bakay, R.A.E., Moore, M.M., Adams, K., and Goldwithe, J. (2000). Direct control of a computer from the human central nervous system. *IEEE Trans. Rehabil. Eng.* 8, 198–202.
- Kennedy, P.R., Kirby, M.T., Moore, M.M., King, B., and Mallory, A. (2004). Computer control using human intracortical local field potentials. *IEEE Trans. Neural Syst. Rehabil. Eng.* 12, 339–344.

- Kim, D.H., and Martin, D.C. (2006). Sustained release of dexamethasone from hydrophilic matrices using PLGA nanoparticles for neural drug delivery. *Biomaterials* 27, 3031–3037.
- Kim, Y.T., Hitchcock, R.W., Bridge, M.J., and Tresco, P.A. (2004). Chronic response of adult rat brain tissue to implants anchored to the skull. *Biomaterials* 25, 2229–2237.
- Kim, S.P., Sanchez, J.C., Rao, Y.N., Erdogmus, D., Carmena, J.M., Lebedev, M.A., Nicolelis, M.A., and Principe, J.C. (2006). A comparison of optimal MIMO linear and nonlinear models for brain-machine interfaces. *J. Neural Eng.* 3, 145–161.
- Kirsch, R.F., Acosta, A.M., van der Helm, F.C., Rotteveel, R.J., and Cash, L.A. (2001). Model-based development of neuroprostheses for restoring proximal arm function. *J. Rehabil. Res. Dev.* 38, 619–626.
- Kovacs, G.T., Stormont, C.W., and Rosen, J.M. (1992). Regeneration microelectrode array for peripheral nerve recording and stimulation. *IEEE Trans. Biomed. Eng.* 39, 893–902.
- Kubler, A., Neumann, N., Kaiser, J., Kotchoubey, B., Hinterberger, T., and Birbaumer, N.P. (2001). Brain-computer communication: Self-regulation of slow cortical potentials for verbal communication. *Arch. Phys. Med. Rehabil.* 82, 1533–1539.
- Kubler, A., Nijboer, F., Mellinger, J., Vaughan, T.M., Pawelzik, H., Schalk, G., McFarland, D.J., Birbaumer, N., and Wolpaw, J.R. (2005). Patients with ALS can use sensorimotor rhythms to operate a brain-computer interface. *Neurology* 64, 1775–1777.
- Kuiken, T. (2006). Targeted reinnervation for improved prosthetic function. *Phys. Med. Rehabil. Clin. N. Am.* 17, 1–13.
- Kurosawa, K., Futami, R., Watanabe, T., and Hoshimiya, N. (2005). Joint angle control by FES using a feedback error learning controller. *IEEE Trans. Neural Syst. Rehabil. Eng.* 13, 359–371.
- Lauer, R.T., Peckham, P.H., and Kilgore, K.L. (1999). EEG-based control of a hand grasp neuroprosthesis. *Neuroreport* 10, 1767–1771.
- Lebedev, M.A., and Nicolelis, M.A.L. (2006). Brain-machine interfaces: Past, present and future. *Trends Neurosci.*, in press.
- Lebedev, M.A., Carmena, J.M., O'Doherty, J.E., Zacksenhouse, M., Henriquez, C.S., Principe, J.C., and Nicolelis, M.A. (2005). Cortical ensemble adaptation to represent velocity of an artificial actuator controlled by a brain-machine interface. *J. Neurosci.* 25, 4681–4693.
- Leuthardt, E.C., Schalk, G., Wolpaw, J.R., Ojemann, J.G., and Moran, D.W. (2004). A brain-computer interface using electrocorticographic signals in humans. *J. Neural Eng.* 1, 63–71.
- Leuthardt, E.C., Schalk, G., Moran, D., and Ojemann, J.G. (2006). The emerging world of motor neuroprosthetics: A neurosurgical perspective. *Neurosurgery* 59, 1–14.
- Lin, S., Si, J., and Schwartz, A.B. (1997). Self-organization of firing activities in monkey's motor cortex: Trajectory computation from spike signals. *Neural Comput.* 9, 607–621.
- Lin, G., Bjornsson, C.S., Smith, K.L., Abdul-Karim, M.-A., Turner, J.N., Shain, W., and Roysam, B. (2005). Automated image analysis methods for 3-D quantification of the neurovascular unit from multichannel confocal microscope images. *Cytometry A* 66, 9–23.
- Liu, X., McCreery, D.B., Carter, R.R., Bullara, L.A., Yuen, T.G., and Agnew, W.F. (1999). Stability of the interface between neural tissue and chronically implanted intracortical microelectrodes. *IEEE Trans. Rehabil. Eng.* 7, 315–326.
- Loeb, G.E., and Davoodi, R. (2005). The functional reanimation of paralyzed limbs. *IEEE Eng. Med. Biol. Mag.* 24, 45–51.
- Loeb, G.E., Bak, M.J., and Duysens, J. (1977). Long-term unit recording from somatosensory neurons in the spinal ganglia of the freely walking cat. *Science* 197, 1192–1194.
- Lu, B., Pang, P.T., and Woo, N.H. (2005). The yin and yang of neurotrophin action. *Nat. Rev. Neurosci.* 6, 603–614.
- Macefield, V.G. (2005). Physiological characteristics of low-threshold mechanoreceptors in joints, muscle and skin in human subjects. *Clin. Exp. Pharmacol. Physiol.* 32, 135–144.
- Malagodi, M.S., Horch, K.W., and Schoenberg, A.A. (1989). An intrascapular electrode for recording of action potentials in peripheral nerves. *Ann. Biomed. Eng.* 17, 397–410.
- Mannard, A., Stein, R.B., and Charles, D. (1974). Regeneration electrode units: Implants for recording from single peripheral nerve fibers in freely moving animals. *Science* 183, 547–549.
- Margalit, E., Weiland, J.D., Clatterbuck, R.E., Fujii, G.Y., Maia, M., Tameesh, M., Torres, G., D'Anna, S.A., Desai, S., Piyathaisere, D.V., et al. (2003). Visual and electrical evoked response recorded from subdural electrodes implanted above the visual cortex in normal dogs under two methods of anesthesia. *J. Neurosci. Methods* 123, 129–137.
- McFarland, D.J., Miner, L.A., Vaughan, T.M., and Wolpaw, J.R. (2000). Mu and beta rhythm topographies during motor imagery and actual movements. *Brain Topogr.* 12, 177–186.
- Meilander, N.J., Yu, X., Ziats, N.P., and Bellamkonda, R.V. (2001). Lipid-based microtubular drug delivery vehicles. *J. Control. Release* 12, 141–152.
- Menei, P., Croue, A., Daniel, V., Pouplardbarthelaix, A., and Benoit, J.P. (1994). Fate and biocompatibility of 3 types of microspheres implanted into the brain. *J. Biomed. Mater. Res.* 28, 1079–1085.
- Mensing, A.F., Anderson, D.J., Buchko, C.J., Johnson, M.A., Martin, D.C., Tresco, P.A., Silver, R.B., and Highstein, S.M. (2000). Chronic recording of regenerating VIIIth nerve axons with a sieve electrode. *J. Neurophysiol.* 83, 611–615.
- Mofid, M.M., Thompson, R.C., Pardo, C.A., Manson, P.N., and VanderKolk, C.A. (1997). Biocompatibility of fixation materials in the brain. *Plast. Reconstr. Surg.* 100, 1420.
- Mohseni, P., Najafi, K., Eliades, S.J., and Wang, X. (2005). Wireless multichannel biopotential recording using an integrated FM telemetry circuit. *IEEE Trans. Neural Syst. Rehabil. Eng.* 13, 263–271.
- Mokry, J., Karbanova, J., Lukas, J., Paleckova, V., and Dvorankova, B. (2000). Biocompatibility of HEMA copolymers designed for treatment of CNS diseases with polymer-encapsulated cells. *Biotechnol. Prog.* 16, 897–904.
- Moxon, K.A., Kalkhoran, N.M., Markert, M., Sambito, M.A., McKenzie, J.L., and Webster, J.T. (2004a). Nanostructured surface modification of ceramic-based microelectrodes to enhance biocompatibility for a direct brain-machine interface. *IEEE Trans. Biomed. Eng.* 51, 881–889.
- Moxon, K.A., Leiser, S.C., Gerhardt, G.A., Barbee, K.A., and Chapin, J.K. (2004b). Ceramic-based multisite electrode arrays for chronic single-neuron recording. *IEEE Trans. Biomed. Eng.* 51, 647–656.
- Najafi, K., Wise, K.D., and Mochizuki, T. (1985). A high-yield IC-compatible multichannel recording array. *IEEE Trans. Elec. Dev.* 32, 1206–1211.
- Neihart, N.M., and Harrison, R.R. (2005). Micropower circuits for bidirectional wireless telemetry in neural recording applications. *IEEE Trans. Biomed. Eng.* 52, 1950–1959.
- Nicolelis, M.A.L., Dimitrov, D., Carmena, J.M., Crist, R., Lehw, G., Kralik, J.D., and Wise, S.P. (2003). Chronic, multisite, multielectrode recordings in macaque monkeys. *Proc. Natl. Acad. Sci. USA* 100, 11041–11046.
- Niedermeyer, E., and Lopes da Silva, F. (1999). *Electroencephalography: Basic Principles, Clinical Applications and Related Fields* (Baltimore: Williams & Wilkins).
- Nunez, P.L., and Srinivasan, R. (2006). *Electric Fields of the Brain: The Neurophysics of EEG* (New York: Oxford University Press).
- Obeid, I., Morizio, J.C., Moxon, K.A., Nicolelis, M.A., and Wolf, P.D. (2003). Two multichannel integrated circuits for neural recording and signal processing. *IEEE Trans. Biomed. Eng.* 50, 255–258.
- Obeid, I., Nicolelis, M.A., and Wolf, P.D. (2004). A low power multichannel analog front end for portable neural signal recordings. *J. Neurosci. Methods* 133, 27–32.
- Paninski, L., Fellows, M.R., Hatsopoulos, N.G., and Donoghue, J.P. (2004). Spatiotemporal tuning of motor cortical neurons for hand position and velocity. *J. Neurophysiol.* 91, 515–532.
- Peckham, P.H., Kilgore, K.L., Keith, M.W., Bryden, A.M., Bhadra, N., and Montague, F.W. (2002). An advanced neuroprosthesis for restoration of hand and upper arm control using an implantable controller. *J. Hand Surg. [Am.]* 27, 265–276.
- Pfurtscheller, G., and Neuper, C. (1997). Motor imagery activates primary sensorimotor area in humans. *Neurosci. Lett.* 239, 65–68.

- Pfurtscheller, G., Graimann, B., Huggins, J.E., Levine, S.P., and Schuh, L.A. (2003). Spatiotemporal patterns of beta desynchronization and gamma synchronization in corticographic data during self-paced movement. *Clin. Neurophysiol.* 114, 1226–1236.
- Polikov, V.S., Tresco, P.A., and Reichart, W.M. (2005). Response of brain tissue to chronically implanted neural electrodes. *J. Neurosci. Methods* 148, 1–18.
- Pouget, A., Zhang, K., Deneve, S., and Latham, P.E. (1998). Statistically efficient estimation using population coding. *Neural Comput.* 10, 373–401.
- Prochazka, A., Westerman, R.A., and Ziccone, S.P. (1976). Discharges of single hindlimb afferents in the freely moving cat. *J. Neurophysiol.* 39, 1090–1104.
- Reier, P., Stensaas, L., and Guth, L. (1983). The astrocytic scar as an impediment to regeneration in the central nervous system. In *Spinal Cord Reconstruction*, C. Kao, R. Bunge, and P. Reier, eds. (New York: Raven Press), pp. 163–195.
- Retterer, S.T., Smith, K.L., Bjornsson, C.S., Neeves, K.B., Spence, A.J.H., Turner, J.N., Shain, W., and Isaacson, M.S. (2004). Model neural prostheses with integrated microfluidics: A potential intervention strategy for controlling reactive cell and tissue responses. *IEEE Trans. Biomed. Eng.* 51, 2063–2073.
- Richardson-Burns, S., Hendricks, J., Sequera, C., Spanninga, S., and Martin, D.C. (2005). Generation of a fully integrated electrode-tissue interface by polymerization of conducting polymer in the presence of living neurons. NIH Neural Interface Workshop, Bethesda, MD.
- Rickert, J., Oliveira, S.C., Vaadia, E., Aertsen, A., Rotter, S., and Mehring, C. (2005). Encoding of movement direction in different frequency ranges of motor cortical local field potentials. *J. Neurosci.* 25, 8815–8824.
- Rojas, A.L., Brockwell, A.E., and Schwartz, A.B. (2005). Improved models for analysis of motor cortical signals. 815. Department of Statistics, Carnegie Mellon University, Pittsburgh, PA.
- Romo, R., Hernandez, A., Zainos, A., Brody, C.D., and Lemus, L. (2000). Sensing without touching: Psychophysical performance based on cortical microstimulation. *Neuron* 26, 273–278.
- Rousche, P.J., and Normann, R.A. (1998). Chronic recording capability of the Utah Intracortical Electrode Array in cat sensory cortex. *J. Neurosci. Methods* 82, 1–15.
- Rubinstein, J.T. (2004). How cochlear implants encode speech. *Curr. Opin. Otolaryngol. Head Neck Surg.* 12, 444–448.
- Salzman, M., and Bak, M.J. (1973). Design fabrication and in vivo behavior of chronic recording intracortical microelectrodes. *IEEE Trans. Biomed. Eng.* 14, 253–260.
- Salinas, E., and Abbott, L.F. (1994). Vector reconstruction from firing rates. *J. Comput. Neurosci.* 1, 89–107.
- Sanes, J.N., and Donoghue, J.P. (1993). Oscillations in local field potentials of the primate motor cortex during voluntary movement. *Proc. Natl. Acad. Sci. USA* 90, 4470–4474.
- Santesteban, F.M.M., Swanson, S.D., Noll, D.C., and Anderson, D.J. (2006). Magnetic resonance compatibility of multichannel silicon microelectrode systems for neural recording and stimulation: Design criteria, tests, and recommendations. *IEEE Trans. Biomed. Eng.* 53, 547–558.
- Schalk, G., Leuthardt, E.C., Moran, D.W., Ojemann, J.G., and Wolpaw, J.R. (2004). Two-dimensional cursor control using electrocorticographic signals in humans. San Diego, CA.
- Scherberger, H., Jarvis, M.R., and Andersen, R.A. (2005). Cortical local field potential encodes movement intentions in the posterior parietal cortex. *Neuron* 46, 347–354.
- Schmidt, E.M. (1999). Electrodes for many single neuron recordings. In *Methods for Neural Ensemble Recordings*, M.A. Nicolelis, ed. (Boca Raton, FL: CRC Press), pp. 1–23.
- Schmidt, E.M., Bak, M.J., and McIntosh, J.S. (1976). Long-term recording from cortical neurons. *Exp. Neurol.* 52, 496–506.
- Schwartz, A.B. (2004). Cortical neural prosthetics. *Annu. Rev. Neurosci.* 24, 487–508.
- Schwartz, A.B., and Moran, D.W. (2000). Arm trajectory and representation of movement processing in motor cortical activity. *Eur. J. Neurosci.* 12, 1851–1856.
- Schwartz, A.B., Kettner, R.E., and Georgopoulos, A.P. (1988). Primate motor cortex and free arm movements to visual targets in three-dimensional space. I. Relations between single cell discharge and direction of movement. *J. Neurosci.* 8, 2913–2927.
- Schwartz, A.B., Taylor, D.M., and Helms-Tillery, S.I. (2001). Extraction algorithms for cortical control of arm prosthetics. *Curr. Opin. Neurobiol.* 11, 701–707.
- Sellers, E.W., and Donchin, E. (2006). A P300-based brain-computer interface: Initial tests by ALS patients. *Clin. Neurophysiol.* 117, 538–548.
- Serruya, M.D., Hatsopoulos, N.G., Paninski, L., Fellows, M.R., and Donoghue, J.P. (2002). Instant neural control of a movement signal. *Nature* 416, 141–142.
- Shain, W., Spataro, L., Dilgen, J., Haverstick, K., Retterer, S., Isaacson, M., Saltzman, M., and Turner, J.N. (2003). Controlling cellular reactive responses around neural prosthetic devices using peripheral and local intervention strategies. *IEEE Trans. Neural Syst. Rehabil. Eng.* 11, 186–188.
- Soechting, J.F. (1983). Kinematics and dynamics of the human arm. 1-17. Laboratory of Neurophysiology, University of Minnesota, Minneapolis, MN.
- Soechting, J.F., and Ross, B. (1984). Psychophysical determination of coordinate representation of human arm orientation. *Neuroscience* 13, 595–604.
- Spataro, L., Dilgen, J., Retterer, S., Spence, A.J., Isaacson, M., Turner, J.N., and Shain, W. (2005). Dexamethasone treatment reduces astroglia responses to inserted neuroprosthetic devices in rat neocortex. *Exp. Neurol.* 194, 289–300.
- Stein, R.B., Charles, D., Davis, L., Jhamandas, J., Mannard, A., and Nichols, T.R. (1975). Principles underlying new methods for chronic neural recording. *Can. J. Neurol. Sci.* 2, 235–244.
- Stein, R.B., Aoyagi, Y., Weber, D.J., Shoham, S., and Normann, R.A. (2004). Encoding mechanisms for sensory neurons studied with a multielectrode array in the cat dorsal root ganglion. *Can. J. Physiol. Pharmacol.* 82, 757–768.
- Stensaas, S.S., and Stensaas, L.J. (1976). The reaction of the cerebral cortex to chronically implanted plastic needles. *Acta Neuropathol. (Berl.)* 35, 187–203.
- Stensaas, S.S., and Stensaas, L.J. (1978). Histopathological evaluation of materials implanted in the cerebral cortex. *Acta Neuropathol. (Berl.)* 41, 145–155.
- Strange, K.D., and Hoffer, J.A. (1999). Restoration of use of paralyzed limb muscles using sensory nerve signals for state control of FES-assisted walking. *IEEE Trans. Rehabil. Eng.* 7, 289–300.
- Suner, S., Fellows, M.R., Vargas-Irwin, C., Nakata, K., and Donoghue, J.P. (2005). Reliability of signals from a chronically implanted, silicon-based electrode array in non-human primate primary motor cortex. *IEEE Trans. Neural Syst. Rehabil. Eng.* 13, 524–541.
- Szarowski, D.H., Andersen, M.D., Retterer, S., Spence, A.J., Isaacson, M., Craighead, H.G., Turner, J.N., and Shain, W. (2003). Brain responses to micro-machined silicon devices. *Brain Res.* 983, 23–35.
- Taylor, D.M., Helms Tillery, S.I., and Schwartz, A.B. (2002). Direct cortical control of 3D neuroprosthetic devices. *Science* 296, 1829–1832.
- Taylor, D.M., Helms Tillery, S.I., and Schwartz, A.B. (2003). Information conveyed through brain-control: Cursor versus robot. *IEEE Trans. Neural Syst. Rehabil. Eng.* 11, 195–199.
- Torebjork, E., Vallbo, A.B., and Ochoa, J.L. (1987). Intraneural microstimulation in man. Its relation to specificity of tactile sensations. *Brain* 110, 1509–1529.
- Turner, J.A., Shain, W., Szarowski, D.H., Andersen, M., Martins, S., Isaacson, M., and Craighead, H. (1999). Cerebral astrocyte response to micromachined silicon implants. *Exp. Neurol.* 156, 33–49.
- Vallbo, A.B. (1981). Sensations evoked from the glabrous skin of the human hand by electrical stimulation of unitary mechanosensitive afferents. *Brain Res.* 215, 359–363.

- Vetter, R.J., Williams, J.C., Hetke, J.F., Nunamaker, E.A., and Kipke, D.R. (2004). Chronic neural recording using silicon-substrate microelectrode arrays implanted in cerebral cortex. *IEEE Trans. Biomed. Eng.* 51, 896–904.
- Voges, J., Waerzeggers, Y., Maarouf, M., Lehrke, R., Koulousakis, A., Lenartz, D., and Sturm, V. (2006). Deep-brain stimulation: Long-term analysis of complications caused by hardware and surgery—experiences from a single centre. *J. Neurol. Neurosurg. Psychiatry* 77, 868–872.
- Wadhwa, R., and Cui, X. (2006). Development of a demand driven drug release system for chronic neural electrode arrays. Annual Meeting of Society for Biomaterials, Pittsburgh, PA.
- Wadhwa, R., Lagenaur, C.F., and Cui, X.T. (2006). Electrochemically controlled release of dexamethasone from conducting polymer polypyrrole coated electrode. *J. Control. Release* 110, 531–541.
- Wahnoun, R., He, J., and Helms Tillery, S.I. (2006). Selection and parameterization of cortical neurons for neuroprosthetic control. *J. Neural Eng.* 3, 162–171.
- Webb, K., Budko, E., Neuberger, T.J., Chen, S., Schachner, M., and Tresco, P.A. (2001). Substrate-bound human recombinant L1 selectively promotes neuronal attachment and outgrowth in the presence of astrocytes and fibroblasts. *Biomaterials* 22, 1017–1028.
- Weber, D.J., Stein, R.B., Everaert, D.G., and Prochazka, A. (2006). Decoding sensory feedback from firing rates of afferent ensembles recorded in cat dorsal root ganglia in normal locomotion. *IEEE Trans. Neural Syst. Rehabil. Eng.* 14, 240–243.
- Weiskopf, N., Mathiak, K., Bock, S.W., Scharnowski, F., Veit, R., Grodd, W., Goebel, R., and Birbaumer, N. (2004). Principles of a brain-computer interface (BCI) based on real-time functional magnetic resonance imaging (fMRI). *IEEE Trans. Biomed. Eng.* 51, 966–970.
- Wessberg, J., Stambaugh, C.R., Kralik, J.D., Beck, P.D., Laubach, M., Chapin, J.K., Kim, J.B.S.J., Srinivasan, M.A., and Nicolelis, M.A.L. (2000). Real-time prediction of hand trajectory by ensembles of cortical neurons in primates. *Nature* 408, 361–365.
- Williams, J.C. (2001). Performance of chronic neural implants: Measurement, modeling and intervention strategies. PhD thesis, Arizona State University, Tempe, Arizona.
- Williams, J.C., Rennaker, R.L., and Kipke, D.R. (1999a). Long-term neural recording characteristics of wire microelectrode arrays implanted in cerebral cortex. *Brain Res. Brain Res. Protoc.* 4, 303–313.
- Williams, J.C., Rennaker, R.L., and Kipke, D.R. (1999b). Stability of chronic multichannel neural recordings: Implications for a long-term neural interface. *Neurocomputing* 26-7, 1069–1076.
- Wilson, J.A., Felton, E.A., Garell, P.C., Schalk, G., and Williams, J.C. (2006). ECoG factors underlying multimodal control of a brain-computer interface. *IEEE Trans. Neural Syst. Rehabil. Eng.* 14, 246–250.
- Wolpaw, J.R., and McFarland, D.J. (2004). Control of a two-dimensional movement signal by a noninvasive brain-computer interface in humans. *Proc. Natl. Acad. Sci. USA* 101, 17849–17854.
- Wu, W., Black, M.J., Mumford, D., Gao, Y., Bienenstock, E., and Donoghue, J.P. (2004). Modeling and decoding motor cortical activity using a switching Kalman filter. *IEEE Trans. Biomed. Eng.* 51, 933–942.
- Wu, W., Gao, Y., Bienenstock, E., Donoghue, J.P., and Black, M.J. (2006). Bayesian population decoding of motor cortical activity using a Kalman filter. *Neural Comput.* 18, 80–118.
- Yoo, S.S., Fairney, T., Chen, N.K., Choo, S.E., Panych, L.P., Park, H., Lee, S.Y., and Jolesz, F.A. (2004). Brain-computer interface using fMRI: Spatial navigation by thoughts. *Neuroreport* 15, 1591–1595.
- Yoshida, K., and Horch, K. (1993). Selective stimulation of peripheral nerve fibers using dual intrafascicular electrodes. *IEEE Trans. Biomed. Eng.* 40, 492–494.
- Yuen, T.G.H., and Agnew, W.F. (1995). Histological-evaluation of polyesterimide-insulated gold wires in brain. *Biomaterials* 16, 951–956.
- Zhong, Y., Yu, X., Gilbert, R., and Bellamkonda, R.V. (2001). Stabilizing electrode-host interfaces: A tissue engineering approach. *J. Rehabil. Res. Dev.* 38, 627–632.